JACS
JOURNAL OF THE AMERICAN CHEMICAL SOCIETY
Communication
pubs.acs.org/JACS

Porous Pt-Ni-P Composite Nanotube Arrays: Highly Electroactive and Durable Catalysts for Methanol Electrooxidation

Liang-Xin Ding, An-Liang Wang, Gao-Ren Li,* Zhao-Qing Liu, Wen-Xia Zhao, Cheng-Yong Su, and Ye-Xiang Tong

MOE Laboratory of Bioinorganic and Synthetic Chemistry, KLGHEI of Environment and Energy Chemistry, School of Chemistry and Chemical Engineering, Instrumental Analysis & Research Center, Sun Yat-sen University, Guangzhou 510275, China

Supporting Information

ABSTRACT: Porous Pt-Ni-P composite nanotube arrays (NTAs) on a conductive substrate in good solid contact are successfully synthesized via template-assisted electrodeposition and show high electrochemical activity and long-term stability for methanol electrooxidation. Hollow nanotubular structures, porous nanostructures, and synergistic electronic effects of various elements contribute to the high electrocatalytic performance of porous Pt-Ni-P composite NTA electrocatalysts.

While great progress has been made toward non-platinum electrocatalysts like functionalized carbon nanotubes/graphenes[1] and non-precious-metal oxides,[2] Pt-based composites are still more efficient electrocatalysts for oxidation of small organic molecules in direct alcohol fuel cells (DAFCs), which are promising power sources for the future.[3−5] Alloying Pt with less expensive 3d-transition metals like Fe, Co, Cu, Mn, or Ni is effective for increasing the electrocatalytic activity and CO tolerance while decreasing Pt consumption, mainly due to the strain and electronic effects between the different components.[6−9] Controllable synthesis of Pt-based composite electrocatalysts has attracted tremendous attention from researchers over the past two decades.

Phosphorus, an inexpensive metalloid element in the same group as nitrogen, has abundant valence electrons, and some studies have focused on the influence of P on the electronic states of metal elements, which have significant effects on, e.g., magnetic and catalytic properties.[10] Incorporating P into Pt-based alloys is highly promising for further enhancing electrocatalytic activities and CO tolerances.[11] However, P is difficult to dope into Pt-based alloys, and the ternary composite of Pt, a non-precious metal, and P as an electrocatalyst for small organic molecule oxidation has been rarely explored.

It is known that the components, morphologies, and crystal structures of electrocatalysts play significant roles in their catalytic activity and durability.[12−16] It has been a huge challenge to realize shape control of Pt−non-precious-metal−P ternary alloy nanocrystals.[11] It has been reported that the addition of P can drastically reduce the size of Pt-based alloy particles,[11] forming small nanocrystals, and accordingly highly ordered Pt-Ni-P composite nanostructures are difficult to synthesize. To our knowledge, the synthesis of 1D Pt-Ni-P composite nanostructures, especially porous nanotube arrays (NTAs), has not been reported until now. Porous Pt-Ni-P composite NTAs are characterized by unique hollow nanostructures, porous structures, anisotropic natures, and multicomponent effects, which impart advantages such as large surface area, high transport rate of electroactive species, high utilization of electrocatalysts, low precious-metal loading, and synergy among the various elements. In addition, well-aligned NTAs may provide continuous charge carrier transport pathways without dead ends. These favorable characteristics will lead to enormous increases in electrocatalytic activity and CO tolerance for Pt-based alloy catalysts.

Based on the above considerations, we synthesized porous Pt-Ni-P composite NTAs with low Pt content by ZnO nanorod array template-assisted electrodeposition, which has the following merits: (i) the orderly porous NTAs are easily synthesized; (ii) P can be easily doped into Pt-Ni alloys; (iii) the porous Pt-Ni-P composite NTAs can grow directly on the conductive substrate in good solid contact, largely enhancing the conductivity. The results we report prove that the porous Pt-Ni-P NTAs exhibit high electrocatalytic activity and durability because of the compositional (i.e., multicomponent composites) and geometrical (i.e., hollow and porous NTA structure) properties of the materials. To our knowledge, this is the first study of methanol electrooxidation on structurally controlled porous Pt-Ni-P composite NTAs.

Scheme 1. Fabrication of Pt-Ni-P NTAs

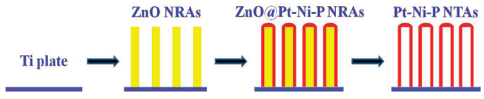

(**NRAs**: nanorod arrays; **NTAs**: nanotube arrays)

The procedure used to fabricate porous Pt-Ni-P NTAs is shown in Scheme 1; it is described in detail in the Supporting Information. Figure 1a shows a typical scanning electron microscopy (SEM) image of Pt-Ni-P NTAs. It is clear that the Pt-Ni-P nanotubes have rough surfaces and lengths of ∼2 μm and are separate from each other. To prove the nanotube structure, Figure 1b shows a typical SEM image of a broken Pt-Ni-P nanotube, with an inner diameter and wall thickness of ∼400 and 70 nm, respectively. The high void volume is also clearly observed in Pt-Ni-P NTAs and will provide a 3D space for mass transfer of reactant and resultant molecules. A typical

Received: December 31, 2011
Published: March 10, 2012

   dx.doi.org/10.1021/ja212206m | J. Am. Chem. Soc. 2012, 134, 5730−5733

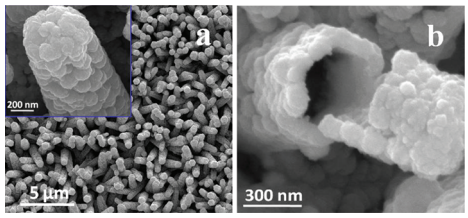

Figure 1. (a) SEM image of Pt-Ni-P NTAs after etching ZnO nanorods and (b) typical SEM image of a broken Pt-Ni-P nanotube.

transmission electron microscopy (TEM) image (Figure 2a) shows that the Pt-Ni-P NTAs have a homogeneous wall

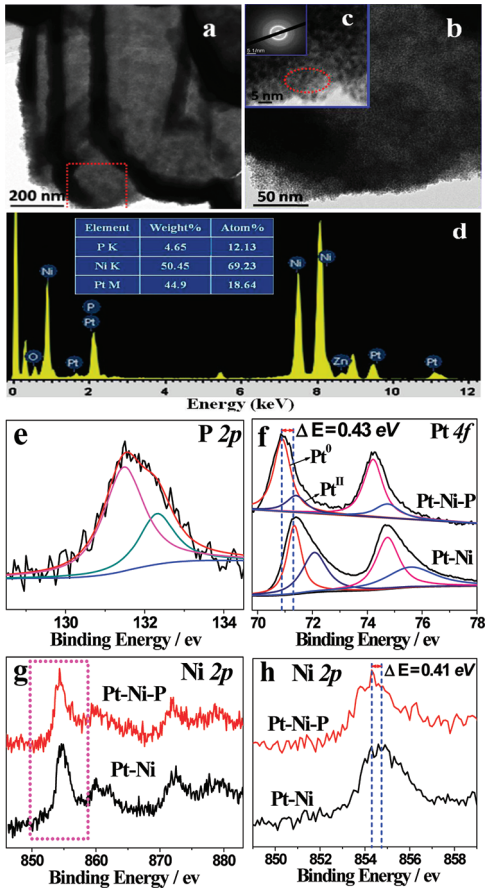

Figure 2. TEM images (a,b), HRTEM image (c), SAED pattern (inset in (c)), and EDS profile (d) of Pt-Ni-P nanotubes. XPS spectra of (e) P 2p, (f) Pt 4f, and (g) Ni 2p [(h) is the magnified spectra of Ni 2p between 849 and 859 eV] for the Pt-Ni-P and Pt-Ni NTAs.

thickness of ~70 nm. A magnified TEM image (Figure 2b) indicates that the nanotube wall is porous and consists of homogeneous overlapped nanocrystals. The Pt-Ni-P nanocrystals range from 3 to 4 nm. The selected area electron diffraction (SAED) pattern of Pt-Ni-P nanotubes (Figure 2c) also indicates that the walls of these nanotubes are polycrystalline and have small size characteristics. The unique porous structure means that the active species can diffuse inside the nanotube walls, and the inner nanocrystals also can efficiently participate in electrocatalytic reactions.

The Pt-Ni-P NTAs were further analyzed by energy-dispersive X-ray spectroscopy (EDS). In the EDS profile of Pt-Ni-P NTAs (Figure 2d), the clear peaks of Pt, Ni and P confirm the successful co-deposition of Pt, Ni, and P. Quantitative analysis from EDS shows 18.64 at% Pt, 69.23 at % Ni, and 12.13 at% P in the Pt-Ni-P nanotubes. The elemental distribution of Pt-Ni-P nanotubes was studied by EDS mapping. Figure S2 reveals that the elements Pt, Ni, and P are homogeneously dispersed in the nanotube wall, representing the homogeneous Pt-Ni-P nanocrystal distribution that will provide a large number of interfaces as active sites for electrocatalytic reactions. For comparison, a Pt-Ni NTAs catalyst was also synthesized by a similar route (Figure S3). The chemical composition of Pt-Ni NTAs was 14.16 at% Pt and 85.84 at% Ni.

Figure 2e–h shows XPS spectra of Pt-Ni-P and Pt-Ni NTAs catalysts in the P 2p, Pt 4f, and Ni 2p regions. The P 2p peaks at 131.5 and 132.3 eV are assigned to P^0 and P^I, respectively (Figure 2e). The peak at 131.5 eV is positively shifted 1.1 eV compared with that of pure phosphorus (130.4 eV). The positive shift of the P 2p peak of P^0 clearly indicates that there is a strong interaction between P, Ni, and Pt. Figure 2f shows the Pt 4f regions of the above two catalysts. Each Pt 4f peak can be deconvoluted into two pairs of doublets. Comparison of the relative areas of integrated intensity of Pt^0 and Pt^{II} shows that plentiful Pt exists as Pt^{II} in the Pt-Ni NTAs catalyst, while only a small amount of Pt^{II} is observed in the Pt-Ni-P NTAs catalyst, indicating that the introduction of P can significantly increase the relative content of Pt^0 in the Pt-Ni-P NTAs catalyst. In addition, we find a definite negative shift of ~0.43 eV in the binding energy of Pt 4f and a slight negative shift of ~0.41 eV in the binding energy of Ni 2p for Pt-Ni-P NTAs relative to Pt-Ni NTAs (Figure 2h). These results further comfirm the electron interactions involving P, Ni, and Pt atoms within Pt-Ni-P NTAs.

The electrochemically active surface area (ECSA) of the catalysts can be calculated from the areas of hydrogen desorption after deduction of the double-layer region. Figure 3a shows the cyclic voltammograms (CVs) of Pt-Ni-P and Pt-Ni NTAs catalysts in N_2-purged 0.5 M H_2SO_4 at a sweep rate of 50 mV/s. The ECSA (m^2/g_{Pt}) of the catalysts is estimated according to the equation[17] ECSA = $Q_H/(210\times W_{Pt})$, where W_{Pt} represents the Pt loading ($\mu g/cm^2$) on the electrode, Q_H is the total charge (μC) for hydrogen desorption, and 210 represents the charge ($\mu C/cm^2_{Pt}$) required to oxidize a monolayer of hydrogen on a bright Pt surface. Herein, the calculated ECSA of Pt-Ni-P NTAs is 28.4 m^2/g_{Pt}, remarkably larger than 3.2 m^2/g_{Pt} for the Pt-Ni NTAs catalyst. Enhancement of the ECSA for Pt-Ni-P NTAs compared with Pt-Ni NTAs may be ascribed to the effect of P on the electronic state of metal elements, the high content of metallic Pt, and the highly uniform dispersion of Pt-Ni-P nanocrystals.

The electrocatalytic properties of Pt-Ni-P versus Pt-Ni NTAs catalysts toward methanol oxidation were investigated in 0.5 M CH_3OH + 0.5 M H_2SO_4. The CVs at 50 mV/s (Figure 3b) show that the specific peak current density of Pt-Ni-P NTAs catalyst is almost 4 times higher than that of Pt-Ni NTAs catalyst (the current densities all are normalized to the ECSA of the catalysts), indicating that the specific electroactivity of the Pt-Ni-P NTAs catalyst is obviously higher than that of the Pt-Ni NTAs catalyst. The onset potential of the forward anodic peak of Pt-Ni-P NTAs is also slightly lower than that of the Pt-Ni NTAs catalyst, indicating that it is more favorable for methanol oxidation on the Pt-Ni-P NTAs. Considering the identical synthetic route and similar Pt content, the much higher electrocatalytic activity of Pt-Ni-P NTAs compared to

dx.doi.org/10.1021/ja212206m | J. Am. Chem. Soc. 2012, 134, 5730–5733

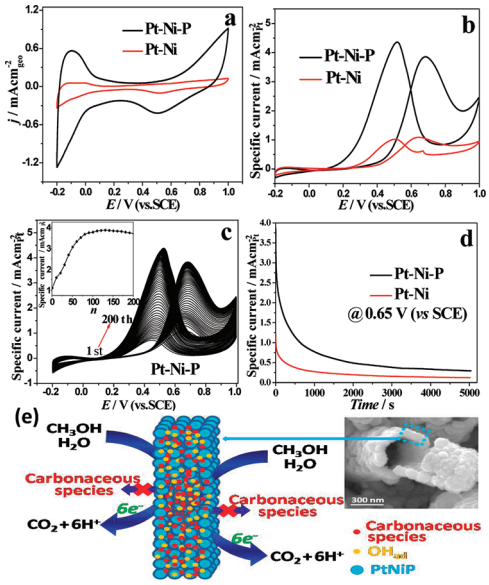

Figure 3. (a) CVs of Pt-Ni-P and Pt-Ni NTAs in 0.5 M H_2SO_4 at 50 mV/s. (b) CVs of Pt-Ni-P and Pt-Ni NTAs in 0.5 M CH_3OH + 0.5 M H_2SO_4 at 50 mV/s. (c) CVs of Pt-Ni-P NTAs catalyst from the 1st to the 200th cycle (inset: change of peak current density with increasing cycle number). (d) Chronoamperometry curves of Pt-Ni-P and Pt-Ni NTAs in 0.5 M H_2SO_4 + 0.5 M CH_3OH at 50 mV/s. (e) Scheme for the almost complete oxidation of carbonaceous species generated during methanol electrooxidation in the porous walls of Pt-Ni-P NTAs.

Pt-Ni NTAs can be mainly ascribed to much larger ECSA and synergetic effects among Pt, Ni, and P.

Figure 3c shows various CVs of Pt-Ni-P NTAs catalyst with increasing cycle number; the inset shows the corresponding change of the peak current density. We find that the catalytic activity of Pt-Ni-P NTAs catalyst increases drastically in the initial cycles. The peak current density reaches a maximum at the 120th cycleand then remains almost stable with increasing cycle number, indicating long-term stability for methanol electrooxidation.

Recently, many publications have reported that the peak current ratio of the forward to backward scans (I_f/I_b) can be used to evaluate the poisoning tolerance of catalysts in DMFCs.[17,18] In this study, we found that the I_f of Pt-Ni-P NTAs catalyst for methanol oxidation increased from 1.04 to 3.85 mA/cm^2 during the initial 120 cycles, while I_f/I_b decreased from 1.43 to 0.88 (Figure 3c). Traditionally, a lower I_f/I_b ratio indicates weaker resistance to poisoning of carbonaceous species. However, here the Pt-Ni-P NTAs catalyst shows high electroactivity and stability. The unique structure of the Pt-Ni-P NTAs catalyst may be a major factor in this contradictory result, because the porous walls of nanotubes can reduce the diffusion rate of the carbonaceous species and lead to complete oxidation of the carbonaceous species during the backward scan (see Figure 3e). Based on the above results, the higher I_b in CVs of Pt-Ni-P NTAs catalyst means less diffusion of carbonaceous species into electrolyte owing to its full oxidation in the porous structures in nanotube walls. Therefore, the special porous structures in the Pt-Ni-P NTAs catalyst can effectively reduce the carbonaceous species "re-occupying" the electroactive sites and consequently enhance the electroactivity and durability.

To further evaluate the rate of surface poisoning, chronoamperometry curves of Pt-Ni-P and Pt-Ni NTAs catalysts were measured in 0.5 M H_2SO_4 + 0.5 M methanol (Figure 3d). The potential was held at 0.65 V during the measurements. It is obvious that the Pt-Ni-P NTAs catalyst exhibits a slower current decay over time in comparison with the Pt-Ni NTAs catalyst, indicating a higher tolerance to the carbonaceous species generated during methanol oxidation. In addition, much higher current densities are seen for the Pt-Ni-P versus the Pt-Ni NTAs catalyst (Figure 3d), indicating that the Pt-Ni-P NTAs catalyst is much more electroactive for methanol oxidation. The above results are consistent with the CV results in Figure 3b.

The electrocatalytic property of the Pt-Ni-P NTAs toward CO oxidation was contrasted with Pt-Ni NTAs in 0.5 M H_2SO_4 electrolyte at room temperature. High-purity CO was bubbled into the electrolyte solution for 15 min while keeping the electrode potential at 0 V to achieve maximum coverage of CO at the Pt centers. Dissolved CO was then purged out of the electrolyte by bubbling Ar gas for 20 min. Two consecutive CVs were recorded for the catalysts between −0.2 and 1.0 V at 50 mV/s (Figure 4). The hydrogen desorption region

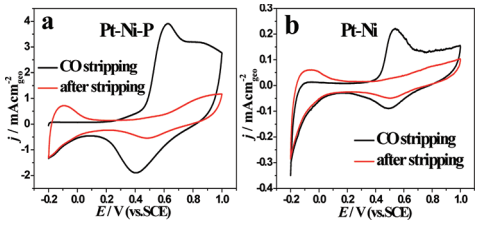

Figure 4. CO stripping measurements of (a) Pt-Ni-P and (b) Pt-Ni NTAs catalysts in 0.5 M H_2SO_4 at 50 mV/s at rt.

disappears in the initial forward scan due to adsorbed CO on the Pt surfaces. A remarkably larger CO oxidation peak is observed on the Pt-Ni-P NTAs catalyst, which could be due to the much larger ECSA of the Pt-Ni-P NTAs catalyst. The onset potential (0.28 V) of CO oxidation on the Pt-Ni-P NTAs catalyst is obviously more negative than that on the Pt-Ni NTAs catalyst (0.36 V) in the first forward scan. This shows that the introduction of P can facilitate removal of CO from the surface of the catalyst, which could be due to P lowering the adsorption strength of CO on the surface of Pt-Ni-P nanocrystals.[19] The disappearance of CO stripping peaks on subsequent scans and reappearance of hydrogen peaks at negative potentials indicate that both catalysts are free of dissolved CO.

In summary, we have designed and synthesized the porous Pt-Ni-P composite NTAs elctrocatalyst by highly efficient template-assisted electrodeposition. We found that the addition of P can effectually lead to a homogeneous nanocrystal size distribution and an enormous increase of the electrochemically active surface areas of Pt-Ni-P NTAs, and also significantly improves the relative content of Pt(0) and the 5d electron density of Pt in Pt-Ni-P NTAs. Moreover, the Pt-Ni-P NTAs take advantage of their unique hollow tubular structure with porous walls for full oxidation of the carbonaceous species generated during methanol electrooxidation, consequently reducing the poisoning of carbonaceous species. The combination of compositionally and geometrically favorable factors provides a new avenue to design electrocatalysts with excellent activity and durability for DMFCs.

dx.doi.org/10.1021/ja212206m | J. Am. Chem. Soc. 2012, 134, 5730−5733

■ ASSOCIATED CONTENT

Supporting Information

Experimental procedure and other information about Pt-Ni-P composite nanotubes. This material is available free of charge via the Internet at http://pubs.acs.org.

■ AUTHOR INFORMATION

Corresponding Author

ligaoren@mail.sysu.edu.cn

Notes

The authors declare no competing financial interest.

■ ACKNOWLEDGMENTS

This work was supported by NSFC (20603048, 51173212, 21073240, and 90923008), Guangdong Province (9251027501000002), Fundamental Research Funds for Central Universities (11lgzd14), and Open-End Fund of State Key Lab of Physical Chemistry of Solid Surfaces (201113).

■ REFERENCES

(1) Wang, S.; Iyyamperumal, E.; Roy, A.; Xue, Y.; Yu, D.; Dai, L. *Angew. Chem., Int. Ed.* **2011**, *50*, 11756. Yang, L.; Jiang, S.; Zhao, Y.; Zhu, L.; Chen, S.; Wang, X.; Wu, Q.; Ma, J.; Ma, Y.; Hu, Z. *Angew. Chem., Int. Ed.* **2011**, *50*, 7132. Wen, Z.; Cui, S.; Pu, H.; Yu, K.; Feng, X.; Chen, J. *Adv. Mater.* **2011**, *23*, 5445. Wang, H.; Liang, Y.; Li, Y.; Dai, H. *Angew. Chem., Int. Ed.* **2011**, *50*, 10969.

(2) Li, Y.; Hasin, P.; Wu, Y. *Adv. Mater.* **2010**, *22*, 1926. Sanabria-Chinchilla, J.; Asazawa, K.; Sakamoto, T.; Yamada, K.; Tanaka, H.; Strasser, P. *J. Am. Chem. Soc.* **2011**, *133*, 5425. Liu, Z.-W.; Peng, F.; Wang, H.-J.; Yu, H.; Zheng, W.-X.; Yang, J. *Angew. Chem., Int. Ed.* **2011**, *50*, 3257.

(3) Wang, L.; Nemoto, Y.; Yamauchi, Y. *J. Am. Chem. Soc.* **2011**, *133*, 9674. Kloke, A.; Stetten, F.; Zengerle, R.; Kerzenmacher, S. *Adv. Mater.* **2011**, *23*, 4976. Wang, R.; Wang, C.; Cai, W.-B.; Ding, Y. *Adv. Mater.* **2010**, *22*, 1845. Xu, C.; Chen, L. Q.; Shen, P. K.; Liu, Y. L. *Electrochem. Commun.* **2007**, *9*, 997. Yang, H. *Angew. Chem., Int. Ed.* **2011**, *50*, 2674. Yang, H.; Zhang, J.; Sun, K.; Zou, S.; Fang, J. *Angew. Chem., Int. Ed.* **2010**, *49*, 6848.

(4) Wang, C.; Tian, W.; Ding, Y.; Ma, Y.; Wang, Z. L.; Markovic, N. M.; Stamenkovic, V. R.; Daimon, H.; Sun, S. *J. Am. Chem. Soc.* **2010**, *132*, 6524. Sun, S.; Zhang, G.; Geng, D.; Chen, Y.; Li, R.; Cai, M.; Sun, X. *Angew. Chem., Int. Ed.* **2011**, *50*, 422. Liang, H.-W.; Cao, X.; Zhou, F.; Cui, C.-H.; Zhang, W.-J.; Yu, S.-H. *Adv. Mater.* **2011**, *23*, 1467. Xu, C. W.; Shen, P. K. *Chem. Commun.* **2004**, 2238. Lim, B.; Yu, T.; Xia, Y. *Angew. Chem., Int. Ed.* **2010**, *49*, 9819. Tian, N.; Zhou, Z.-Y.; Sun, S.-G.; Ding, Y.; Wang, Z. L. *Science* **2007**, *316*, 732.

(5) Zhou, Z.-Y.; Huang, Z.-Z.; Chen, D.-J.; Wang, Q.; Tian, N.; Sun, S.-G. *Angew. Chem., Int. Ed.* **2010**, *49*, 411. Wu, J.; Zhang, J.; Peng, Z.; Yang, S.; Wagner, F. T.; Yang, H. *J. Am. Chem. Soc.* **2010**, *132*, 4984. Lim, B.; Lu, X.; Jiang, M.; Camargo, P. C.; Cho, E. C.; Lee, E. P.; Xia, Y. *Nano Lett.* **2008**, *8*, 4043. Gao, M.-R.; Gao, Q.; Jiang, J.; Cui, C.-H.; Yao, W.-T.; Yu, S.-H. *Angew. Chem., Int. Ed.* **2011**, *50*, 4905.

(6) Zhang, J.; Yang, H.; Yang, K.; Fang, J.; Zou, S.; Luo, Z.; Wang, H.; Bae, I.-T.; Jung, D. Y. *Adv. Funct. Mater.* **2010**, *20*, 3727. Zhang, X.-B.; Yan, J.-M.; Han, S.; Shioyama, H.; Xu, Q. *J. Am. Chem. Soc.* **2009**, *131*, 2778. Hsieh, C.-T.; Lin, J.-Y. *J. Power Sources* **2009**, *188*, 347.

(7) Jiang, S.; Ma, Y.; Jian, G.; Tao, H.; Wang, X.; Fan, Y.; Lu, Y.; Hu, Z.; Chen, Y. *Adv. Mater.* **2009**, *21*, 4953. Liu, L.; Pippel, E.; Scholz, R.; Gösele, U. *Nano Lett.* **2009**, *9*, 4352. Dubau, L.; Durst, J.; Maillard, F.; Guétaz, L.; Chatenet, M.; André, J.; Rossinot, E. *Electrochim. Acta* **2011**, *56*, 10658. Ji, X.; Lee, K. T.; Holden, R.; Zhang, L.; Zhang, J.; Botton, G. A.; Couillard, M.; Nazar, L. F. *Nat. Chem.* **2010**, *2*, 286.

(8) Xu, D.; Liu, Z.; Yang, H.; Liu, Q.; Zhang, J.; Fang, J.; Zou, S.; Sun, K. *Angew. Chem., Int. Ed.* **2009**, *48*, 4217. Srivastava, R.; Mani, P.; Hahn, N.; Strasser, P. *Angew. Chem., Int. Ed.* **2007**, *46*, 8988. Shao, M.; Shoemaker, K.; Peles, A.; Kaneko, K.; Protsailo, L. *J. Am. Chem. Soc.* **2010**, *132*, 9253.

(9) Kang, Y.; Murray, C. B. *J. Am. Chem. Soc.* **2010**, *132*, 7568. Xu, C.; Su, Y.; Tan, L.; Liu, Z.; Zhang, J.; Chen, S.; Jiang, S. P. *Electrochim. Acta* **2009**, *54*, 6322. Alayoglu, S.; Zavalij, P.; Eichhorn, B.; Wang, Q.; Frenkel, A. I.; Chupas, P. *ACS Nano* **2009**, *3*, 3127. Wanjala, B. N.; Fang, B.; Luo, J.; Chen, Y.; Yin, J.; Engelhard, M. H.; Loukrakpam, R.; Zhong, C.-J. *J. Am. Chem. Soc.* **2011**, *133*, 12714.

(10) Wonterghem, J. V.; Morup, S.; Christion, J. W.; Charles, S.; Wells, W. S. *Nature* **1986**, *322*, 622. Luo, G.; Yan, S.; Qiao, M.; Fan, K. *J. Mol. Catal. A* **2005**, *230*, 69. King, W. D.; Corn, J. D.; Murphy, O. J.; Boxall, D. L.; Kenik, E. A.; Kwiatkowski, K. C.; Stock, S. R.; Lukehart, C. M. *J. Phys. Chem. B* **2003**, *107*, 5467. Daimon, H.; Kurobe, Y. *Catal. Today* **2006**, *111*, 182.

(11) Xue, X.; Ge, J.; Liu, C.; Xing, W.; Lu, T. *Electrochem. Commun.* **2006**, *8*, 1280. Xue, X.; Ge, J.; Tian, T.; Liu, C.; Xing, W.; Lu, T. *J. Power Sources* **2007**, *172*, 560.

(12) Xu, C.; Wang, L.; Wang, R.; Wang, K.; Zhang, Y.; Tian, F.; Ding, Y. *Adv. Mater.* **2009**, *21*, 2165. Wang, C.; Chi, M.; Strmcnik, D.; Vliet, D.; Wang, G.; Komanicky, V.; Chang, K.-C.; Paulikas, A. P.; Tripkovic, D.; Pearson, J.; More, K. L.; Markovic, N. M.; Stamenkovic, V. R. *J. Am. Chem. Soc.* **2011**, *133*, 14396. Chen, Z.; Waje, M.; Li, W.; Yan, Y. *Angew. Chem., Int. Ed.* **2007**, *46*, 4060. Liu, L.; Pippel, E. *Angew. Chem., Int. Ed.* **2011**, *50*, 2729.

(13) Mohanty, A.; Garg, N.; Jin, R. *Angew. Chem., Int. Ed.* **2010**, *49*, 4962. Alia, S. M.; Zhang, G.; Kisailus, D.; Li, D.; Gu, S.; Jensen, K.; Yan, Y. *Adv. Funct. Mater.* **2010**, *20*, 3742. Koenigsmann, C.; Santulli, A. C.; Gong, K.; Vukmirovic, M. B.; Zhou, W.; Sutter, E.; Wong, S. S.; Adzic, R. R. *J. Am. Chem. Soc.* **2011**, *133*, 9783. Kwon, Y.; Lai, S. C. S.; Rodriguez, P.; Koper, M. T. M. *J. Am. Chem. Soc.* **2011**, *133*, 6914. Strmcnik, D.; Escudero-Escribano, M.; Kodama, K.; Stamenkovic, V. R.; Cuesta, A.; Marković, N. M. *Nat. Chem.* **2010**, *2*, 880.

(14) Liu, Z.; Jackson, G. S.; Eichhorn, B. W. *Angew. Chem., Int. Ed.* **2010**, *49*, 3173. Wang, C.; Chi, M.; Li, D.; Strmcnik, D.; Vliet, D.; Wang, G.; Komanicky, V.; Chang, K.-C.; Paulikas, A. P.; Zhang, D. H.; Jin, M.; Wang, J.; Li, W.; Camargo, P. H. C.; Kim, M. J.; Yang, D.; Xie, Z.; Xia, Y. *J. Am. Chem. Soc.* **2011**, *133*, 6078. Cui, C.-H.; Li, H.-H.; Yu, J.-W.; Gao, M.-R.; Yu, S.-H. *Angew. Chem., Int. Ed.* **2010**, *49*, 9149.

(15) Lim, B.; Xia, Y. *Angew. Chem., Int. Ed.* **2011**, *50*, 76. Nilekar, A. U.; Sasaki, K.; Farberow, C. A.; Adzic, R. R.; Mavrikakis, M. *J. Am. Chem. Soc.* **2011**, *133*, 18574. Guo, S.; Dong, S.; Wang, E. *ACS Nano* **2010**, *4*, 547. Yoo, E.; Okata, T.; Akita, T.; Kohyama, M.; Nakamura, J.; Honma, I. *Nano Lett.* **2009**, *9*, 2255. Zhou, Z.-Y.; Huang, Z.-Z.; Chen, D.-J.; Wang, Q.; Tian, N.; Sun, S.-G. *Angew. Chem., Int. Ed.* **2010**, *49*, 411. Carmo, M.; Sekol, R. C.; Ding, S.; Kumar, G.; Schroers, J.; Taylor, A. D. *ACS Nano* **2011**, *5*, 2979.

(16) Hwang, S. J.; Yoo, S. J.; Jang, S.; Lim, T.-H.; Hong, S. A.; Kim, S.-K. *J. Phys. Chem. C* **2011**, *115*, 2483. Wanjala, B. N.; Fang, B.; Luo, J.; Chen, Y.; Yin, J.; Engelhard, M. H.; Loukrakpam, R.; Zhong, C.-J. *J. Am. Chem. Soc.* **2011**, *133*, 12714. RodriguezP.KwonY.KoperM. T. M.Nat. Chem.2012ChuehW. C.HaoY.JungW.HaileS. M.Nat. Mater.2012

(17) Liu, L.; Pippel, E.; Scholz, R.; Gösele, U. *Nano Lett.* **2009**, *9*, 4352.

(18) Wen, Z. H.; Wang, Q.; Li, J. H. *Adv. Funct. Mater.* **2008**, *18*, 959. Tiwari, J. N.; Pan, F.-M.; Lin, K.-L. *New J. Chem.* **2009**, *33*, 1482. Y. Lin, H.; Cui, X. L.; Yen, C.; Wai, C. M. *J. Phys. Chem. B* **2005**, *109*, 14410. Liu, F.; Lee, J. Y.; Zhou, W. J. *Small* **2006**, *2*, 121.

(19) Yang, G.; Chen, Y.; Zhou, Y.; Tang, Y.; Lu, T. *Electrochem. Commun.* **2010**, *12*, 492.